AGU PUBLICATIONS

Paleoceanography

RESEARCH ARTICLE
10.1002/2013PA002574

Key Points:
- Coccolithophores record orbital-suborbital climate changes at the mid-Brunhes
- Key taxa highlight glacial-interglacial front dynamics at Site MD01-2446
- Coccolithophores as proxy for recognition of Heinrich-type events

Correspondence to:
M. Marino,
maria.marino@uniba.it

Citation:
Marino, M., P. Maiorano, F. Tarantino, A. Voelker, L. Capotondi, A. Girone, F. Lirer, J.-A. Flores, and B. D. A. Naafs (2014), Coccolithophores as proxy of seawater changes at orbital-to-millennial scale during middle Pleistocene Marine Isotope Stages 14–9 in North Atlantic core MD01-2446, *Paleoceanography*, *29*, 518–532, doi:10.1002/2013PA002574.

Received 7 NOV 2013
Accepted 3 APR 2014
Accepted article online 9 APR 2014
Published online 12 JUN 2014

Coccolithophores as proxy of seawater changes at orbital-to-millennial scale during middle Pleistocene Marine Isotope Stages 14–9 in North Atlantic core MD01-2446

Maria Marino[1], Patrizia Maiorano[1], Francesca Tarantino[1], Antje Voelker[2,3], Lucilla Capotondi[4], Angela Girone[1], Fabrizio Lirer[5], José-Abel Flores[6], and B. David A. Naafs[7]

[1]Dipartimento di Scienze della Terra e Geoambientali, Università degli Studi di Bari Aldo Moro, Bari, Italy, [2]Divisão de Geologia e Georecursos Marinhos, Instituto Português do Mar e da Atmosfera, Lisbon, Portugal, [3]CIMAR Associated Laboratory, Porto, Portugal, [4]Istituto di Scienze Marine, CNR, Bologna, Italy, [5]Istituto Ambiente Marino Costiero, CNR, Naples, Italy, [6]Departamento de Geología, Grupo de Geociencias Oceánicas (GGO), Universidad de Salamanca, Salamanca, Spain, [7]School of Chemistry, Organic Geochemistry Unit, and Cabot Institute, University of Bristol, Bristol, UK

Abstract Quantitative coccolithophore analyses were performed in core MD01-2446, located in the midlatitude North Atlantic, to reconstruct climatically induced sea surface water conditions throughout Marine Isotope Stages (MIS) 14–9. The data are compared to new and available paleoenvironmental proxies from the same site as well as other nearby North Atlantic records that support the coccolithophore signature at glacial-interglacial to millennial climate scale. Total coccolithophore absolute abundance increases during interglacials but abruptly drops during the colder glacial phases and deglaciations. Coccolithophore warm water taxa (wwt) indicate that MIS11c and MIS9e experienced warmer and more stable conditions throughout the whole photic zone compared to MIS13. MIS11 was a long-lasting warmer and stable interglacial characterized by a climate optimum during MIS11c when a more prominent influence of the subtropical front at the site is inferred. The wwt pattern also suggests distinct interstadial and stadial events lasting about 4–10 kyr. The glacial increases of *Gephyrocapsa margereli-G. muellerae* 3–4 μm along with higher values of C_{org}, additionally supported by the total alkenone abundance at Site U1313, indicate more productive surface waters, likely reflecting the migration of the polar front into the midlatitude North Atlantic. Distinctive peaks of *G. margereli-muellerae* (>4 μm), *C. pelagicus pelagicus*, *Neogloboquadrina pachyderma* left coiling, and reworked nannofossils, combined with minima in total nannofossil accumulation rate, are tracers of Heinrich-type events during MIS12 and MIS10. Additional Heinrich-type events are suggested during MIS12 and MIS14 based on biotic proxies, and we discuss possible iceberg sources at these times. Our results improve the understanding of mid-Brunhes paleoclimate and the impact on phytoplankton diversity in the midlatitude North Atlantic region.

1. Introduction

The middle Pleistocene Marine Isotope Stages (MIS) 14–9 include the mid-Brunhes [*Jansen et al.*, 1986; *Barker et al.*, 2006], which is a crucial time of important global climate change when, following the mid-Pleistocene transition, glacial-interglacial cyclicity became more stable at the periodicity of about 100 kyr [*Berger and Wefer*, 2003]. Interglacial phases were warmer starting from MIS 11 [*Jansen et al.*, 1986; *Lisiecki and Raymo*, 2005] and the amplitude of glacial terminations is greater since 450 ka (Terminations I–V) [*Lang and Wolff*, 2011]. A distinctive interval of the mid-Brunhes is the interglacial MIS 11 that is considered the longest-lasting warmer interglacial of the last 1.0 Ma [*McManus et al.*, 1999; *Hodell et al.*, 2000]. MIS 11 is depicted as a potential analog of the Holocene [*Howard*, 1997; *Loutre and Berger*, 2003; *de Abreu et al.*, 2005] and follows the largest amplitude transition (Termination V) of the last 500 ka [*Oppo et al.*, 1998]. The glacial MIS 12 is indeed known to be the strongest of the last 800 ka in agreement with an array of proxy evidence from marine, ice core, and terrestrial archives [*Lang and Wolff*, 2011]. On the other hand, MIS 14 was a particularly weak glacial [*Tzedakis et al.*, 2006; *Lüthi et al.*, 2008], with reduced ice sheet volume, absence of Hudson Strait Heinrich (-like) events in the North Atlantic [*Naafs et al.*, 2013], relative higher sea level, and higher sea surface and atmospheric temperatures with respect to the younger glacials [*Lisiecki and Raymo*, 2005; *Bintanja et al.*, 2005]. Deglaciation toward MIS 13 (Termination VI) was of low amplitude with values well below those

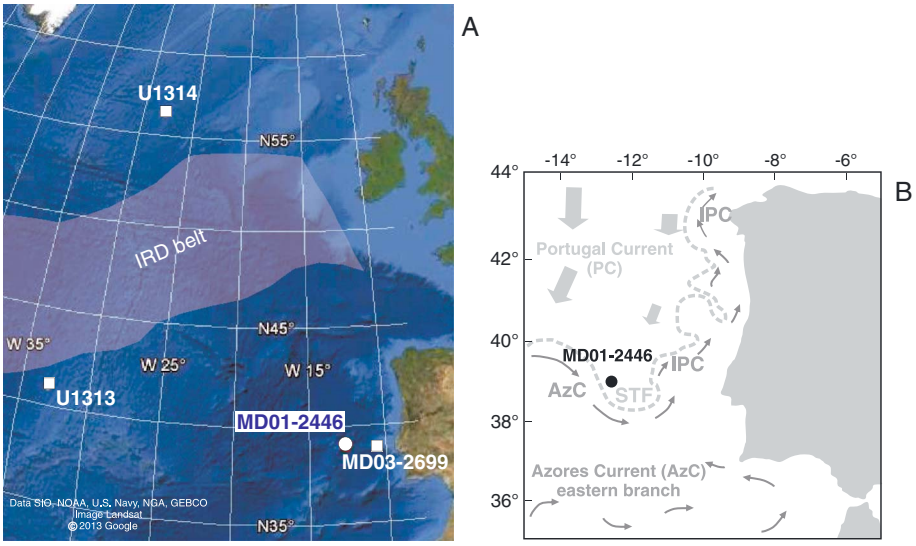

Figure 1. (a) Location map of the studied core MD01-2446 and other sites mentioned in the text. (b) Surface water circulation during winter is redrawn from *Voelker et al.* [2010] according to *Peliz et al.* [2005]. IPC = Iberian Poleward Current. STF = subtropical front. Ice-rafted detritus (IRD) belt is drawn according to *Ruddiman* [1977] for the last glacial period.

recorded at the Terminations IV and V [*Lang and Wolff*, 2011]. Previous data suggest a minimum of ice volume during MIS 13, particularly during substage MIS 13a [*Lisiecki and Raymo*, 2005; *Jouzel et al.*, 2007].

Furthermore, the mid-Brunhes interval is characterized by abrupt and rapid climate changes both during glacials and interglacials (stadials and interstadials, Heinrich (H)-type events) as evidenced by sharp shifts in the sea surface temperature (SST), biomarker-derived paleoproductivity, magnetic susceptibility, distinctive abundance pattern of the polar foraminifer *Neogloboquadrina pachyderma* left coiling, and from sudden variation in stable carbon and oxygen isotope records. This is widely documented in recent studies that have focused on the occurrence of H-type events and related ice-rafted detritus (IRD) throughout the mid-Brunhes glacials down to MIS 16 in North Atlantic records from the middle to high latitudes [*Oppo et al.*, 1998; *McManus et al.*, 1999; *Martrat et al.*, 2007; *Hodell et al.*, 2008; *Stein et al.*, 2009; *Voelker et al.*, 2010; *Rodrigues et al.*, 2011; *Naafs et al.*, 2011, 2013; *Alonso-Garcia et al.*, 2011] and within the Mediterranean Sea [*Girone et al.*, 2013]. It is in fact established that high-frequency climate perturbations first recognized in the last glacial cycle [*Broecker et al.*, 1992; *Bond et al.*, 1992; *Rohling et al.*, 1998; *Cacho et al.*, 1999, 2001; *de Abreu et al.*, 2003; *Hemming*, 2004; *Sierro et al.*, 2005; *Voelker et al.*, 2006; *Salgueiro et al.*, 2010] persisted through the middle Pleistocene. Data from IODP (Integrated Ocean Drilling Program) Site U1313 [*Hodell et al.*, 2008; *Stein et al.*, 2009; *Naafs et al.*, 2011, 2013] and cores MD01-2446 [*Voelker et al.*, 2010] and MD03-2699 [*Voelker et al.*, 2010; *Rodrigues et al.*, 2011] highlight that the effects of North Atlantic ice sheet instability were recorded at wider latitudinal scale and well beyond the IRD belt defined by *Ruddiman* [1977] for the last glacial period (Figure 1).

In recent years a few studies [*Incarbona et al.*, 2008; *Amore et al.*, 2012; *Bordiga et al.*, 2013a, 2013b; *Girone et al.*, 2013; *Maiorano et al.*, 2013a, 2013b; *Palumbo et al.*, 2013] investigated the response of the coccolithophore assemblages and variations in their absolute abundance to such climate changes during the mid-Brunhes. Coccolithophores represent a major component of marine primary producers and are sensitive to rapid and abrupt fluctuations in temperature, salinity, nutrients, and turbidity of surface waters [*McIntyre and Bè*, 1967; *Baumann et al.*, 2005]. They are mainly used as valuable tool for paleoclimate and paleoceanographic reconstruction since they are abundant in deep-sea sediments and widespread in the oceans, with distinct bioprovince distributions controlled by latitudinal oceanic zonation and frontal system dynamics [*McIntyre and Bè*, 1967; *Bown et al.*, 2004; *Ziveri et al.*, 2004]. Coccolithophores are mostly *K* selected, adapted to oligotrophic conditions, and benefit from warm and stable surface waters. However, they also include specific taxa having peculiar ecological preference for more eutrophic or rapidly changing conditions and thus are particularly usable for detailed paleoenvironmental reconstructions [*Baumann et al.*, 2005].

Our study therefore aims to reconstruct orbital (glacial-interglacial) to short-term millennial-scale (e.g., H-type) climate changes during the interval from MIS 14 to 9 based on coccolithophores as powerful proxy of sea surface water conditions. We use quantitative analyses in samples from midlatitude North Atlantic core MD01-2446 (Figure 1), located in an area sensitive to record subtropical and subpolar front dynamics. The acquired coccolithophore absolute abundances and derived paleoecological indices are compared to IRD, benthic, and planktonic $\delta^{18}O$ and $\delta^{13}C$ records [*Voelker et al*., 2010] (here extended to the lower MIS 8), the new quantitative data collected on *Neogloboquadrina pachyderma* left coiling and the $CaCO_3$ content. Finally, data of core MD01-2446 are compared to the other paleoceanographic records from the North Atlantic (IODP Sites U1313 and U1314, core MD03-2699) with the aim to correlate coccolithophore-based signals of abrupt and short-term surface water changes at the study site with well-known and widespread events of iceberg discharge from the Laurentide and European ice sheets. New data on alkenones/TOC (total organic carbon) are also provided for Site U1313, since it is a midlatitude open ocean North Atlantic reference section [*Naafs et al*., 2012, 2013] recording climate changes similar to those of core MD01-2446.

2. Study Area and Oceanographic Setting

The studied Calypso giant piston core MD01-2446 (39°03.36'N, 12°37.44'W) was retrieved on the southeastern slope of the Tore Seamount, about 300 km west of Portugal (Figure 1a) at a water depth of 3547 m, with R/V *Marion Dufresne* during the MD123-Geosciences cruise in 2001. Modern surface water characteristics at the core location are mainly influenced by the Portugal Current (PC) and the Azores Current (AzC) (Figure 1b). The PC forms in the Northeastern Atlantic as a recirculation of the North Atlantic Current [*Peliz et al*., 2005] and moves southward along the Iberian margin (Figure 1b). The AzC derives from the Gulf Stream and flows in large meanders eastward between 35 and 37°N through the midlatitude North Atlantic (eastern branch shown in Figure 1b). The AzC's northern boundary forms the subtropical front (STF). The Iberian Poleward Current (IPC) (Figure 1b) originates from the AzC and, including a subsurface component of less ventilated, warm, and saltier waters of subtropical origin, moves northward during winter [*Peliz et al*., 2005]. Upwelling of subsurface components of PC and IPC waters occurs north of 45°N and south of 40°N, respectively, but depending on strong wind systems upwelling of subpolar subsurface waters might also occur south of 40°N. At present the site is bathed by Northeast Atlantic Deep Water (NEADW), but the efficiency and strength of NEADW production varied with glacial-interglacial cycles as Antarctic Bottom Water (AABW) flowed farther north during glacials [*Raymo et al*., 1997; *Voelker et al*., 2010]. The core location is at the southern edge of the North Atlantic IRD belt [*Ruddiman*, 1977; *Hemming*, 2004], as reconstructed for the last glacial period, where large SST shifts occurred during glacials [*Pflaumann et al*., 2003] and stadials [*Chapman and Maslin*, 1999; *Oppo et al*., 2001; *Salgueiro et al*., 2010]. However, more recent high-resolution data documented the presence of meltwater and IRD in the midlatitude North Atlantic throughout the middle Pleistocene interval (MIS 9-14/16) [*Stein et al*., 2009; *Voelker et al*., 2010; *Rodrigues et al*., 2011; *Naafs et al*., 2013] and in the Mediterranean Sea [*Girone et al*., 2013].

North Atlantic Sites IODP U1313 and U1314 and core MD03-2699 (Figure 1a), selected for comparison with our data, are from oceanographic settings valuable to record changes in water mass boundary dynamics. Today Site U1313 is mainly influenced by the warm and oligotrophic surface waters of the North Atlantic Current, but in the past it sometimes was located at the southern boundary of the Ruddiman IRD belt receiving IRD mainly from the Laurentide ice sheet via iceberg discharge through Hudson Bay [*Stein et al*., 2009; *Naafs et al*., 2011, 2013]. IODP Site U1314, located within the subpolar North Atlantic Ocean, is strongly influenced by the North Atlantic Current and able to record changes in the surface circulation of the subpolar gyre and abrupt pulses of IRD mainly from Greenland and Iceland ice sheet sources [*Alonso-Garcia et al*., 2011]. The location of core MD03-2699, offshore off Portugal, is influenced by the same water masses as core MD01-2446 and provides additional information on orbital to suborbital climate changes in the region [*Voelker et al*., 2010; *Rodrigues et al*., 2011].

3. Age Model and Biochronology

In this paper the age model and marine oxygen isotope stratigraphy of core MD01-2446 developed by *Voelker et al*. [2010] for the interval MIS 13 to lower MIS 9 was extended into early MIS 8 (Figure 2). The age model was established by correlating the benthic oxygen isotope curve of MD01-2446 with the benthic record at IODP Site U1313 for the interval from MIS 13 to lower MIS 10 [*Voelker et al*., 2010] and with the stack

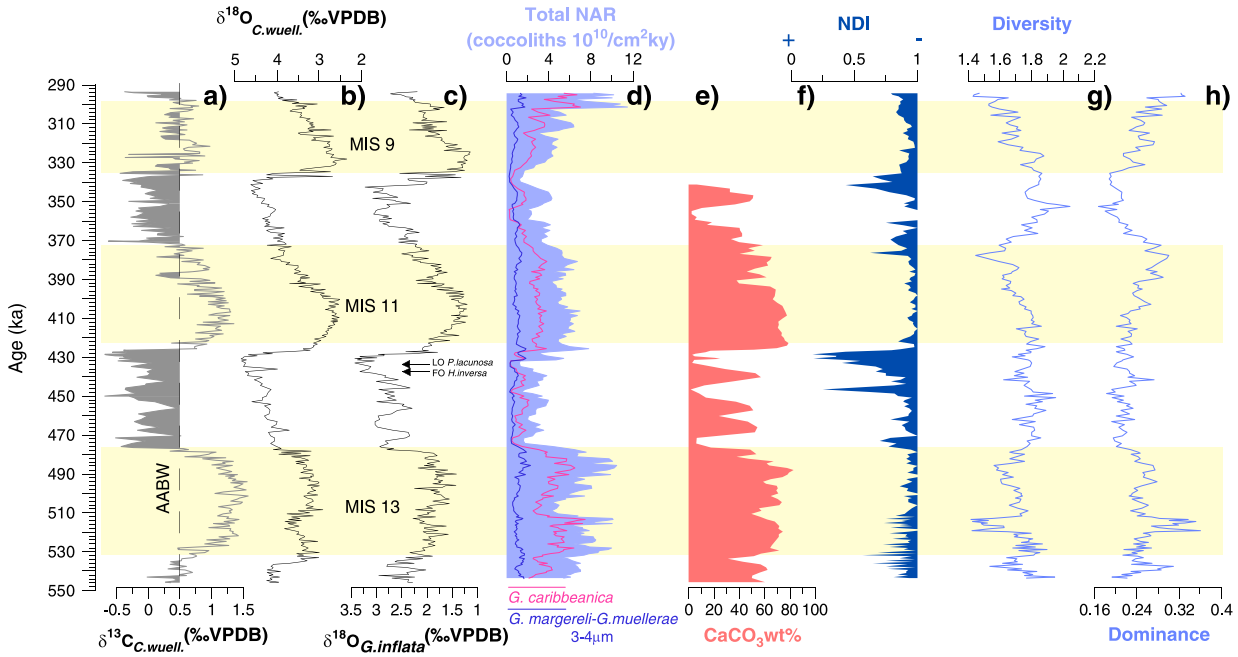

Figure 2. (a–c) Oxygen and carbon isotope records are from *Voelker et al.* [2010] and this paper. (d) Total coccolith accumulation rate (NAR), correlated with (e) $CaCO_3$, (f) nannofossil dissolution index (NDI), (g) coccolithophore diversity, and (h) dominance indices. LO: last occurrence. FO: first occurrence. Yellow bars highlight interglacial stages according to chronology of *Lisiecki and Raymo* [2005]. Marine Isotope Stages (MIS) are indicated.

record of *Lisiecki and Raymo* [2005] for late MIS 10 to lower MIS 8 [*Voelker et al.*, 2010; this study], with isotopic maxima providing most correlation points. On average sedimentation rates vary from 2 to 3.5 cm/ka; higher values are recorded during MIS 13 (3.5–4.5 cm/ka), at the MIS 12/11 transition (5.7 cm/ka), and in the lower MIS 8 (5 cm/ka).

The age model is supported by biochronology of the last occurrence (LO) of *Pseudoemiliania lacunosa* at 1715 cm with an age assignment of 436.67 ka (Figure 2), which is well comparable to the ages of 436 ka and 440 ka recorded in the Pacific and Atlantic Oceans, respectively [*Raffi et al.*, 2006; *Hagino and Kulhanek*, 2009]. A slightly older age of 452.47 ka has recently been estimated by *Amore et al.* [2012] for the LO of *P. lacunosa* in nearby core MD03-2699. An additional bioevent is the local first occurrence of *Helicosphaera inversa* at 439 ka (1716.5 cm) in the uppermost MIS 12 slightly below the LO of *P. lacunosa* (Figure 2). Comparable distribution of the species was found in the Mediterranean Sea [*Maiorano et al.*, 2013b] and at Site U1313 [*Hagino and Kulhanek*, 2009]. On the contrary, an older first occurrence (FO) [*Amore et al.*, 2012] of the taxon (514 ka) was indicated at core MD03-2699, possibly in relation to different hydrological setting and position of the latter core south of STF with respect to the studied site during the investigated interval (Figure 1).

4. Methods

4.1. Coccolithophore Analysis and Taxonomic Remarks

Samples from Core MD01-2446 were taken from 1253 to 2050 cm, corresponding to the upper MIS 14 to lower MIS 8 (294.2–543.58 ka). The coccolithophore assemblages were analyzed in 228 samples with a spacing of about 2–4 cm between 514 ka and 543 ka (1943–2050 cm) and 4–5 cm for the remaining part, providing a temporal resolution of about 0.6–0.8 kyr and of 0.8 to 1.2 kyr, respectively. As in the midlatitude North Atlantic abrupt and rapid SST fluctuations, referred as H-type events, last about 2.4 kyr to 4.5/7 kyr during MIS 15–9 [*Rodrigues et al.*, 2011], the adopted time resolution enables us to investigate millennial-scale climate changes.

Slides for coccolithophore analysis were prepared according to the method of *Flores and Sierro* [1997], which makes it possible to estimate absolute coccolith abundances. Quantitative analyses were performed using a polarized light microscope at 1000X magnification. Abundances were determined by counting 500 coccoliths

of all sizes in a variable number of visual fields generally ranging from 4 to 6 in samples from interglacial periods to 10–16 in glacial samples. The specimens of reworked nannofossils were counted separately. In each sample additional area was scanned, up to 30 fields of view (about 1 mm^2), in order to detect uncommon and rare taxa. This supplementary counting was necessary due to the gephyrocapsid dominance that may prevent the recognition of rare taxa useful in paleoenvironmental reconstruction. About 36 taxa were identified at species and subspecies level. Quantitative data on the coccolithophore assemblages were computed using the software PAST (Paleontology Statistics) [*Hammer et al*., 2001] to estimate ecological indices: (i) Diversity, taking into account the number of individuals and the number of taxa, varies from zero (when the assemblage is represented by only one taxon) to higher values that increase with the number of taxa and the individuals of each taxon becoming equally abundant within the assemblage and (ii) dominance, a measure of the relative importance of one taxon within the assemblage.

Variations in the abundance of coccoliths were estimated using percentages and nannofossil accumulation rates (NAR), calculated according to *Flores and Sierro* [1997]. We used the wet bulk density (shipboard natural gamma ray density data) instead of the dry bulk density since the latter is not available for the core. Therefore, the NAR (coccoliths × cm^{-2} × kyr^{-1}) is derived from N × w × S, where N = coccolith/g of sediment, w = wet bulk density (g/cm^3), and S = sedimentation rate (cm/kyr). NAR is a proxy of paleoproductivity [*Steinmetz*, 1994; *Baumann et al*., 2004] although it may depend on the changeable surface water condition that may favor/inhibit the proliferation of coccolithophores [*Flores et al*., 1997; *Kinkel et al*., 2000; *Baumann et al*., 2005; *Stolz and Baumann*, 2010], on dilution process due to variable sedimentation rates and amount of terrigenous input, and on dissolution.

An estimate of coccolith dissolution (NDI) was obtained using the method of *Marino et al*. [2009]. High values of NDI indicate good preservation. A similar index was used by other authors [*Matsuoka*, 1990; *Dittert et al*., 1999; *Boeckel and Baumann*, 2004; *Bordiga et al*., 2013a] to estimate nannofossil dissolution in different ocean basins.

Taxonomy of *Gephyrocapsa*, which represents the major component of the assemblages, follows the criteria adopted in *Maiorano et al*. [2013a]. Specifically, gephyrocapsids with closed central area are indicated as *Gephyrocapsa caribbeanica*; gephyrocapsids with open central area, here indicated as *Gephyrocapsa margereli-Gephyrocapsa muellerae*, include *Gephyrocapsa* generally 3–4 μm in size with a bridge angle between 25 and 40°. Rare to very rare specimens having bridge angles <25° (*Gephyrocapsa muellerae*) or slightly higher than 40° (*Gephyrocapsa oceanica*) were also recognized and included in this group since they were not unambiguously distinguishable under the polarized light microscope. Specimens of *G. margereli-G. muellerae* >4 μm were also discriminated.

4.1.1. Coccolithophore Indicators for Paleoproductivity and Paleotemperature

Primary productivity of the upper photic zone (*N* index = NI) was calculated according to *Flores et al*. [2000]: NI = small placoliths <4 μm/(small placoliths <4 μm + *Florisphaera profunda*). The NI ratio is used as a proxy for primary productivity since small placoliths are abundant in the upper photic zone with intense upwelling and high primary productivity [*Wells and Okada*, 1997; *Okada and Wells*, 1997; *Beaufort et al*., 1997]. *F. profunda* on the other hand, a deep dweller photic zone taxon, is abundant in coccolithophore assemblages when the nutricline/thermocline is deep [*Molfino and McIntyre*, 1990a, 1990b; *McIntyre and Molfino*, 1996; *Beaufort et al*., 1997, 2001; *Di Stefano and Incarbona*, 2004]. High NI values indicate a shallow nutricline/thermocline and upwelling. Although *F. profunda* is rare in the studied core, similar to other Atlantic and Pacific records, the NI ratio is considered a quite useful proxy of paleoproductivity.

The cumulative abundances of the taxa *Syracosphaera histrica*, *S. pulchra*, *Rhabdosphaera clavigera*, *R. clavigera* var. *stylifera*, *Umbilicosphaera sibogae*, *U. foliosa*, *Calciosolenia* spp., *Oolithotus* spp. (mostly *O. antillarum*), and *Umbellosphaera* spp. (mainly *U. tenuis*) are considered as warm-water proxy (wwt) at site MD01-2446. Although these taxa show significant fluctuations, they record low abundance throughout the record even within the supplementary fields of view, in general, ranging from 5 to 20 specimens during glacials and up to 60–90 specimens during interglacials. Each of these taxa displays values not higher than 2.5%, with *Syracosphaera* spp. and *Oolithotus* spp. as the main contributors. These wwt are known to have an affinity with oligotrophic tropical-subtropical oceanic water masses [*McIntyre and Bè*, 1967; *Winter et al*., 1994; *Ziveri et al*., 1995, 2004; *Baumann et al*., 2004; *Boeckel and Baumann*, 2004; *Saavedra-Pellitero et al*., 2010; *Palumbo et al*., 2013], and therefore, their distinctive increases can be considered as indicator of warmer and oligotrophic surface water and the presence of tropical-subtropical water at the core location. Among the

wwt, the distribution of *Umbellosphaera* spp., despite its very low abundance, was also used to further infer environmental condition within the photic zone. *Umbellosphaera* spp. prefers tropical-subtropical oligotrophic waters [*Kinkel et al*., 2000; *Okada and McIntyre*, 1979]. *U. tenuis* is a characteristic species of oligotrophic conditions and thrives within the middle photic zone [*Honjo and Okada*, 1974; *Cortes et al*., 2001; *Cros*, 2001; *Haidar and Thierstein*, 2001; *Dimiza and Triantaphyllou*, 2010] where it benefits from the lower light intensity level that usually occur between 50 m and 75 m water depth [*Cortes et al*., 2001]. *U. irregularis* is considered one of the most oligotrophic coccolithophore species [*Cortes et al*., 2001]. High abundances of *Umbellosphaera* spp. (up to 70% of the assemblages) were found in living assemblages from the oligotrophic waters of the equatorial Atlantic where the genus is reported as abundant at intermediate depth (50–100 m) [*Kinkel et al*., 2000]. This taxon is used to infer well-developed oligotrophic conditions down to the middle of the photic zone.

We consider *G. margereli-G. muellerae* as indicators of cool/cold surface water condition with *G. muellerae* being the "cold" gephyrocapsid of *Bollmann* [1997], in agreement with several other studies [*Weaver and Pujol*, 1988; *Samtleben and Bickert*, 1990; *Okada and Wells*, 1997; *Saavedra-Pellitero et al*., 2010; *Amore et al*., 2012] and *G. margereli* the gephyrocapsid typical of transitional assemblages [*Bollmann*, 1997]. Living *G. muellerae* is mainly found in the eastern North Atlantic, north of 50°N and south of the Iceland-Scotland Ridge (10–30°W) [*Giraudeau et al*., 2010]. Larger morphotypes of *G. margereli-G. muellerae* (>4 μm) are used as a signal of colder and low-salinity water influx during abrupt glacial episodes of iceberg melting. This idea is sustained by the occurrence of larger morphotypes of *G. margereli-G. muellerae* (>4 μm) documented in the Mediterranean Sea during the glacial MIS 12 and 10 [*Girone et al*., 2013] related to abrupt influx of cold Atlantic waters into the Mediterranean Basin via the Strait of Gibraltar during nearly synchronous North Atlantic H-type events. An affinity for lower temperatures was established in several studies for larger-sized Noelaerhabdaceae specimens of gephyrocapsids [*Kulhanek et al*., 2008; *Kulhanek*, 2009; *Girone et al*., 2013] and *Emiliania huxleyi* [*Colmenero-Hidalgo et al*., 2002, 2004; *Sierro et al*., 2005; *Sorrosa et al*., 2005; *Flores et al*., 2010].

C. pelagicus pelagicus is used as an indicator of polar-subpolar meltwater influx at the site location. The taxon is considered a subarctic species [*Baumann et al*., 2000; *Geisen et al*., 2002] that benefits from colder condition [*Okada and McIntyre*, 1979; *Winter et al*., 1994]. It is found together with high abundances of *N. pachyderma* left coiling and related to the influx of subpolar waters off western Iberia during Heinrich events of the last 200 ka [*Parente et al*., 2004]. Similarly, increases of *C. pelagicus pelagicus* have been recorded at core MD03-2699 during H-type events within MIS 12 [*Amore et al*., 2012]. Furthermore, distinct glacial short-term peaks in the pattern of *C. pelagicus pelagicus* during the mid-Pleistocene transition have been observed just prior to IRD peaks at the northern Atlantic ODP Site 980 [*Marino et al*., 2011].

4.2. *Neogloboquadrina pachyderma* Left Coiling

The percentage of the planktonic foraminifer *N. pachyderma* left coiling was counted in samples from the same depth as those studied for the coccolithophore assemblages. Quantitative abundance was obtained in the residue >150 μm. The residue was split to obtain a representative aliquot containing about 300 specimens, and all specimens were counted in the aliquot. Species abundance was quantified as percentages within the total number of planktonic foraminifers. *N. pachyderma* left coiling is a polar-subpolar taxon [*Hemleben et al*., 1989; *Bé and Tolderlund*, 1971; *Reynolds and Thunell*, 1986; *Johannessen et al*., 1994], and peak abundances of the taxon often are coincident with abrupt drops in SST and low salinity and with peaks of IRD. The taxon is used to recognize polar-subpolar (melt)water influx at the study site, linked to H-type events, in agreement with previous studies [*Bond et al*., 1992; *Broecker et al*., 1992; *Oppo et al*., 1998; *Cacho et al*., 1999; *Perez-Folgado et al*., 2003; *Sierro et al*., 2005].

4.3. Stable Isotopes and Sediment Geochemistry

New stable isotope analyses in 23 additional samples from the younger section (1253–1332 cm, upper MIS 9 and lower MIS 8) were performed using the benthic foraminifer *Cibicidoides wuellerstorfi* and the planktonic foraminifer *Globorotalia inflata*, respectively. The methodology for these analyses is the same as described in *Voelker et al*. [2010]. The stable isotopes of *G. inflata* shell reflect conditions in the winter mixed layer [*Deuser and Ross*, 1989] as recorded at the base of the thermocline [*Cléroux et al*., 2007]. During most time intervals *G. inflata* records the same conditions as surface dwelling foraminifer species but with a dampened signal [*Voelker et al*., 2009; *Voelker and de Abreu*, 2011]. New data on $CaCO_3$ and C_{org} are presented for core MD01-2446,

together with new records on alkenones pattern at Site U1313. The $CaCO_3$ and C_{org} contents were determined for the core interval between 1400 cm and 2057 cm (between 341 kyr and 545 kyr). Two milligrams of dried, ground, and homogenized total sediment were processed, using the CHNS-932 Leco element analyzer of the Marine Geology Laboratory at LNEG (Amadora, Portugal). The values, expressed as weight percent (wt %), are based on three repeated analyses (with precision ±0.5), and the temporal resolution ranges from 0.7 to 2 ka.

The alkenone analyses from 690 samples of IODP Site U1313 are provided with a temporal resolution of about 0.2–0.4 ka. Alkenone data are expressed as μg/g of TOC following the methods described in *Stein et al*. [2009] and *Naafs et al*. [2011], and they are interpreted as indicator of marine surface water productivity [*Villanueva et al*., 1997; *Stein et al*., 2009; *Naafs et al*., 2010].

All raw and derived data reported against age have been deposited on PANGAEA data server (www.pangaea.de).

5. Results and Discussion

5.1. Pattern of Coccolith Production

The NAR of total coccoliths varies from 1.2×10^{10} to 12×10^{10} (Figure 2d). The assemblages are mainly composed of *Gephyrocapsa caribbeanica* (correlation = 0.85 with dominance, Figure 2h) that reaches higher abundance during interglacials (Figure 2d). The *G. margereli-G. muellerae* group is also a major component of the assemblages with percentages as high as 35%. The positive correlation between the pattern of total NAR and $\delta^{18}O_{G.inflata}$ both at glacial-interglacial and millennial scale (Figures 2c and 2d) suggests a strict relation with temperature as the primary control factor for the proliferation of coccolithophore assemblages at the site location. The high positive correlation observed between total NAR and $CaCO_3$ (Figures 2d and 2e) reveals that coccoliths-derived carbonate is the major contributor to carbonate production at site MD01-2446. This is not surprising for the mid-Brunhes marine carbonates that mainly originated from a wide-scale dominance of *G. caribbeanica* [*Baumann and Freitag*, 2004]. The cooccurrence of high-dissolution intervals recorded within glacial MIS 12 and 10 (Figure 2f) and lower total NAR, and $CaCO_3$ values are likely the result of a more efficient northward penetration of the carbonate corrosive AABW at the site location during glacial cycles [*Oppo and Lehman*, 1993; *Raymo et al*., 2004; *Martrat et al*., 2007; *Voelker et al*., 2010] as also testified by the minima in benthic $\delta^{13}C$ (Figure 2a). On the other hand, minima in diversity (Figure 2g) do not match the NDI ($r = -0.08$); therefore, with the exception of restricted dissolution intervals within MIS 12 and in the upper MIS 10 (Figure 2f), the assemblage variations through time can be considered as a signal of primary response of coccolithophores to paleoenvironmental changes.

5.2. Interglacial Phases

The distinct increases of warm and oligotrophic water taxa (wwt) during MIS 13c and throughout MIS 11 and MIS 9 (Figure 3d) imply prominent sea surface warming and relatively stable interglacial conditions at these times with respect to glacials, according to *Voelker et al*. [2010]. The wwt curve strictly mimics the shape of the planktonic $\delta^{18}O$ fluctuations both at glacial/interglacial and stadial/interstadial scales (Figures 3b and 3d). Two distinct positive wwt increases correlate with MIS 11c and MIS 11a and with MIS 9e and MIS 9a–9c (Figures 3b and 3d), and they are concurrent with higher total NAR (Figure 3c), suggesting that coccolithophore assemblages benefit from the warm and stable oligotrophic condition during interglacials. Concurrent lower values in NI may be observed during interglacials (Figure 3i), with the exception of MIS 13. In detail, during MIS 13c the wwt record millennial-scale variability and high values (comparable to those recorded in the younger interglacials) while the distribution of *F. profunda*, which has a minimum temperature limit at about 10–12°C [*Okada and Honjo*, 1973], shows very low abundances with respect to MIS 11 and MIS 9 (Figure 3f). This suggests that the water warming in the photic zone likely affected only the upper surface waters during MIS 13c while more unstable conditions, according to *Voelker et al*. [2010], occurred in the thermocline waters, where *F. profunda* may thrive. On the other hand, the observed low abundances of wwt during MIS13a, considered the warmest substage within MIS 13 [*Jouzel et al*., 2007; *Lisiecki and Raymo*, 2005; *Bintanja et al*., 2005], may imply that higher nutrients in the surface water would have been unfavorable to the proliferation of wwt. The $\delta^{13}C_{G.\ inflata}$ values, which are at their maximum during MIS 13a (Figure 3a) possibly in relation to condition of mixing and upwelling of cool and nutrient-rich waters [*Voelker et al*., 2010], support this interpretation. Higher fluctuations of total NAR together with higher

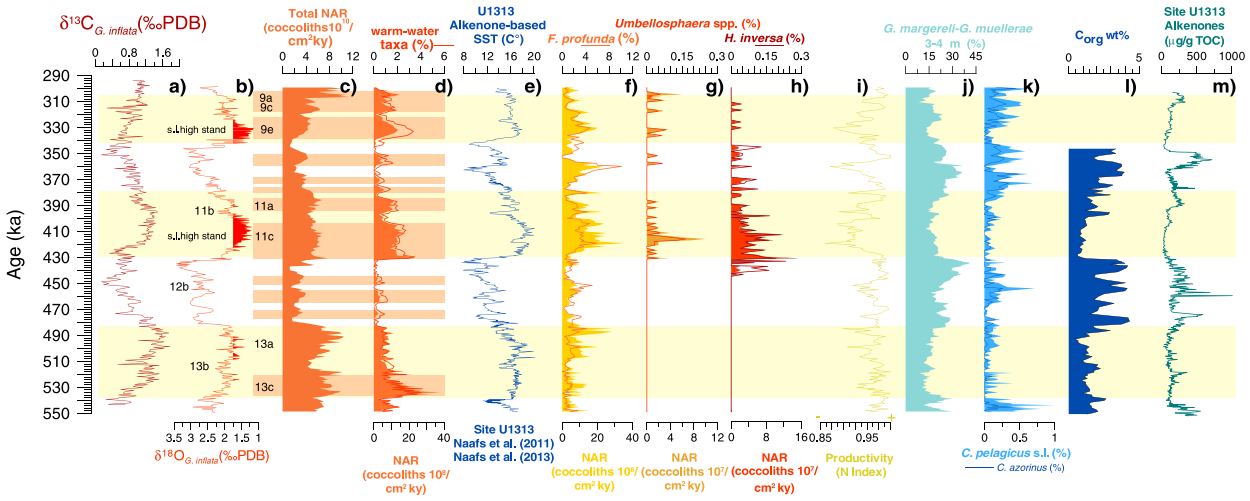

Figure 3. (a and b) Oxygen and carbon isotope records [*Voelker et al*., 2010, and this paper] are correlated with (c) total NAR, (d) warm-water taxa, (f, h, j, and k) selected coccolithophores, (i) *N* index, and (l) C_{org} values. (m) Total alkenone concentration (µg/gTOC) and (e) alkenone-based sea surface temperature (SST) [*Stein et al*., 2009; *Naafs et al*., 2011] profile of IODP Site U1313 are also shown. Yellow bars as in Figure 2; orange bars highlight short-term increases of warm-water taxa; substages are according to *Tzedakis et al*. [1997] for MIS 11 and MIS 9, and as in *Voelker et al*. [2010] for MIS 13.

NI (Figure 3i) during MIS 13 (Figure 3c) also sustain higher surface water instability. These results provide further evidence of more unstable conditions during MIS 13 than the subsequent counterparts [*Hodell et al*., 2003; *Voelker et al*., 2010; *Rodrigues et al*., 2011; *Lang and Wolff*, 2011].

At site MD01-2446 an abrupt increase of wwt is recorded at 426 ka close to the MIS 12/MIS 11 transition (Termination V (TV)), and it has a time lag of about 2 kyr with respect to the earliest sharp decrease in the $\delta^{18}O_{G.\ inflata}$ values (428 ka), the latter reflecting the effect of reduced salinity related to the rapid and strong deglaciation at the TV, following the most severe glacial of the last half million years [*Oppo et al*., 1998; *Howard*, 1997]. In contrast, the true surface water warming is marked by the increase of wwt that is contemporaneous with the increase of the total NAR (Figure 3c) and with the abrupt increase in the SST at Site U1313 (Figure 3e), located farther west [*Stein et al*., 2009; *Naafs et al*., 2011, 2013]. A within error bars simultaneous warming (at 426.6 ka) is also recorded in the SST curve of core MD03-2699 (see Figure 4) [*Rodrigues et al*., 2011] indicating a wide-scale midlatitude North Atlantic surface water warming. The observed wwt increase at the Termination IV (TIV) was less abrupt than at the MIS 12/11 shift, in agreement with the SST pattern at Site U1313 (Figures 3d and 3e), and it does not coincide, as at TV, with the first decrease in $\delta^{18}O_{G.inflata}$ (Figure 3b). These results suggest that the wwt curve is a reliable signal of surface water temperature change in the studied sector of the North Atlantic Ocean and that TV was more extreme than TIV. On the other hand, the slightly gradual wwt increase associated with Termination VI (TVI) highlights a less intense deglaciation at this time when neither salinity-related abrupt lowering in the $\delta^{18}O$ curve (Figure 3b) nor a high-amplitude change in temperature (Figure 3e) occurred.

Further insight into the description of MIS 11 and 9 (Figures 3f–3h) may be pointed out based on the distinctive distribution of selected rare taxa. *F. profunda* mostly shows distinct increases during MIS 11c and 9e, although percentages never exceed 6% (Figure 3f). In contrast *H. inversa* and *Umbellosphaera* spp. (Figures 3g and 3h) mostly occurred during MIS 11. *Umbellosphaera* spp. has a distinct peak of absolute abundance during MIS 11c, suggesting well-developed oligotrophic conditions down to the middle of the photic zone. These conditions are likely related to the prolonged period of stable warm-water conditions during this interval. The higher absolute abundance of *H. inversa*, a species that thrived in warm surface waters and whose distribution seems affected by surface water masses and hydrographic fronts, in the substage MIS 11c (Figure 3h) is likely an indication of a more prominent influence of the subtropical front at the core location during MIS 11, as discussed in *Maiorano et al*. [2013b]. The taxon was also documented in the Ionian Sea during a climate optimum nearly coincident with substage MIS 11c [*Maiorano et al*., 2013b] and well comparable with a climate optimum of wide significance in the North Atlantic [i.e., *Helmke et al*., 2008; *Kandiano et al*., 2012]. The cooccurrence of higher absolute abundances of *H. inversa*, *Umbellosphaera*

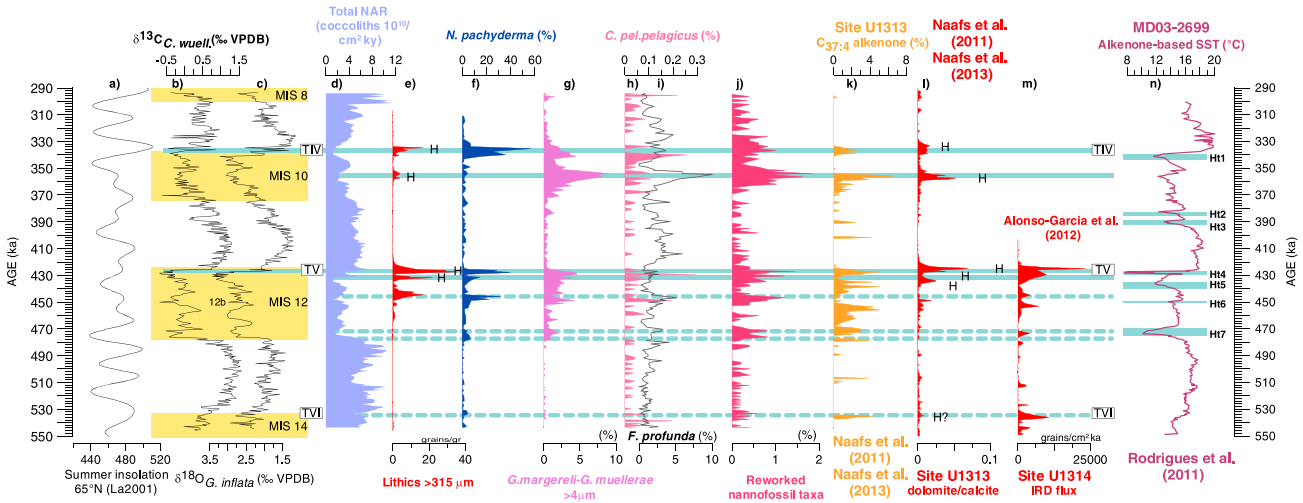

Figure 4. (a) Summer insolation curve at 65°N [*Laskar et al.*, 2004] and (b and c) oxygen and carbon isotope records [*Voelker et al.*, 2010, and this paper] correlated with (d) total NAR, (e) lithics concentration [*Voelker et al.*, 2010], (f) abundance pattern of *N. pachyderma* left coiling, and (g–j) selected coccolithophore indicators of (k) core MD01-2446. Proxies of meltwater influx ($C_{37:4}$ alkenones) and (l and m) of ice-rafted detritus (dolomite/calcite and IRD flux) during Heinrich-type events (H) at IODP sites U1313 [*Stein et al.*, 2009; *Naafs et al.*, 2011] and U1314 [*Alonso-Garcia et al.*, 2012] are shown. (n) Heinrich-type events (Ht1–Ht7) and alkenone-based SST curve of core MD03-2699 are also indicated according to *Rodrigues et al.* [2011]. Heinrich-type events are marked by light blue bands; dashed lines highlight additional H-type events inferred in the present study. Terminations (T) IV, V, and VI are indicated. Yellow bars on the left indicate glacial phases according to chronology of *Lisiecki and Raymo* [2005].

spp., and *F. profunda* during MIS 11c (Figure 3) is consistent with this climate optimum and, according to the ecology of the last two taxa, indicates higher temperatures in both surface and subsurface waters, coupled with a more stratified and oligotrophic water column, occurred at this time. Coccolithophore data correlate well with the first phase (404–418 ka) of sea level highstand/warmth highlighted by *Voelker et al.* [2010] (red area in Figure 3b) and combined with the wwt pattern supports the hypothesis that MIS 11 was the warmest long-lasting and stable interglacial of the investigated record [*Hodell et al.*, 2000; *Droxler et al.*, 2003; *Loutre and Berger*, 2003; *McManus et al.*, 2003; *de Abreu et al.*, 2005; *Jouzel et al.*, 2007; *Tzedakis*, 2010; *Voelker et al.*, 2010]. Our data could also be a signal of a northward transport of tropical/subtropical waters toward the location of core MD01-2446, in agreement with data from several North Atlantic Ocean sites [*de Abreu et al.*, 2005; *Martrat et al.*, 2007; *Helmke et al.*, 2008; *Hagino and Kulhanek*, 2009; *Stein et al.*, 2009; *Voelker et al.*, 2010; *Rodrigues et al.*, 2011; *Kandiano et al.*, 2012].

5.3. Glacial Intervals

Higher-frequency climate variability is limited to glacials. In detail, based on the wwt pattern, three interstadials can be traced in glacial MIS 12 and 10 (Figure 3d), which indicate events lasting about 4–10 kyr. The colder phases of glacial MIS 12 and 10 (Figure 3j) are characterized by considerable percentage abundance of *G. margereli-G. muellerae* 3–4 μm, corresponding to lower total NAR and heavier values of $\delta^{18}O$ (Figures 3b and 3c), and low temperatures at Site U1313 (Figure 3e). The higher abundances of *G. margereli-G. muellerae* 3–4 μm (Figures 3j and 3k) during lower total NAR and C_{org} increase (Figures 3c and 3l) may imply that the taxon was also able to thrive in cold and high productive surface waters (higher NI values, Figure 3i) during glacial episodes. Such a decrease of total NAR is likely the result of lower coccolith abundance in the sediment that develops under nutrient-rich surface water conditions (possibly upwelling related) [*Lebreiro et al.*, 1997], which may have restrained production of many coccolithophores that are adapted to oligotrophic conditions [*Baumann et al.*, 2004, 2005]. At Site U1313 the total alkenone concentration (Figure 3m) [*Stein et al.*, 2009, and this paper] further supports higher primary productivity during cold periods, mainly linked to *Gephyrocapsa* proliferation [*Marlowe et al.*, 1990], *G. margereli-G. muellerae* in our record. At the studied site, the influx of nutrient-rich water and subsequent enhanced surface coccolithophore productivity could have been favored by southward migration of the polar front during glacials [*Villanueva et al.*, 2001], in agreement with the reconstruction of a polar front position near to Site U1313 during MIS 12 and 10 as suggested by *Stein et al.* [2009]. The decrease of total NAR at these times could

be a signal of lower $CaCO_3/C_{org}$ rain ratio during glacials [*Archer and Maier-Reimer*, 1994; *Sigman et al*., 1998; *Munhoven*, 2007] although a possible effect of dissolution cannot be excluded in the upper MIS 12 (see NDI pattern in Figure 2f). Furthermore, it is likely that during glacials noncalcifying prymnesiophytes, among the phytoplanktonic organisms [e.g., *Di Tullio et al*., 2000; *Tortell et al*., 2002], could have mostly contributed to enhancing of alkenones, while diatoms to C_{org} increase. The suggested glacial paleoenvironmental conditions at the location of core MD01-2446 are in agreement with higher glacial productivity documented at the same site during the last three glacials [*Lebreiro et al*., 1997; *Nave et al*., 2010].

The significant contribution of *C. pelagicus azorinus* within *Coccolithus pelagicus* s.l. during glacials and above MIS 9e (Figure 3k) could indicate an influence of water masses from the AzC (Figure 1b) and periods of intensified upwelling [*Parente et al*., 2004] at the core location.

5.4. Millennial-Scale Climate Variability During Glacials

The millennial-scale climate changes, mainly linked to H-type events at site MD01-2446, have been documented by *Voelker et al*. [2010] during MIS 12 and 10 based on abundance peaks of lithic fragments (>315 μm) interpreted as IRD. This data set may be extended by looking at the pattern of NAR and selected coccolithophore taxa, and percentage of *N. pachyderma* left coiling, a species classically linked to Heinrich (-like) events in this region. As expected, the major peaks of *N. pachyderma* left coiling (Figure 4f) are mostly in phase with peaks of lithics at the core location (Figure 4e). The significant total NAR decreases, concomitant to IRD layers (Figure 4d), are consistent with unfavorable (cold, turbid, and low salinity) surface water condition for coccolithophore productivity [*Stolz and Baumann*, 2010], even though a possible dilution effect caused by high-detritus input cannot be excluded, as it is the case at TV, which records the highest sedimentation rate (5.7 cm/ka) throughout the core. *G. margereli-G. muellerae* >4 μm (Figure 4g) have distinct increases during restricted intervals of MIS 12 and 10, similarly to the subarctic *C. pelagicus pelagicus*, which also shows short-term peaks during MIS 14 and 8 (Figure 4h). The more prominent peaks of *G. margereli-G. muellerae* >4 μm and *C. pelagicus pelagicus* slightly preceded the major peaks of lithic fragments at core MD01-2446 ("H" on lithics curve in Figure 4e). In addition, they cooccurred with a rapid shift toward lower planktonic $\delta^{18}O$ and $\delta^{13}C$ values (Figure 4) at the TIV and TV, suggesting lower surface water salinity. This may imply that *G. margereli-G. muellerae* >4 μm and *C. pelagicus pelagicus* were able to benefit from surface conditions just preceding the IRD discharge. Synchronous SST minima and $C_{37:4}$ maxima and enhanced phytoplankton productivity [*Stein et al*., 2009] recorded at Site U1313 just before the occurrence of the main IRD peaks (Figures 4k and 4l) are in agreement with the present results. In core MD01-2446, the IRD peaks during MIS 10 (including TIV) and TV match the abundance peaks of reworked nannofossil taxa (Figure 4j). The latter may indicate the real timing of iceberg-derived detritus release and consequent turbid surface waters, which resulted in unfavorable condition for *G. margereli-G. muellerae* >4 μm and *C. pelagicus pelagicus*. The taxa in fact record minor to major decreases concomitant to the peaks of lithics. A singular major peak in the pattern of *F. profunda* is coincident with the H-type event recorded at about 356 ka within MIS 10 (Figure 4i) and simultaneous with a minimum in NI (see Figure 3i) and a prominent peak of reworking (Figure 4j). A possible reason for the distinct pattern of the taxon may be linked to enhanced and abrupt water stratification and warmer subsurface water at the thermocline/nutricline depth, below a cold freshwater and possibly turbid lid determined by meltwater discharge, in agreement with condition of an inverse thermocline during H(-like) events [*Colmenero-Hidalgo et al*., 2004], although it does not appear to be a common feature of all the recorded H-type events.

The H-type events during MIS 10 and at TV in core MD01-2446 are also recorded at Sites U1313 [*Stein et al*., 2009; *Naafs et al*., 2011, 2013] and U1314 [*Alonso-Garcia et al*., 2011] (Figure 4m). They coincide with insolation maxima (Figure 4a), which have been proposed as forcing mechanism for ice sheet instability, melting, and iceberg discharge [*Stein et al*., 2009]. Based on our biotic proxies, similar environmental conditions can be inferred at supplementary levels and specifically within MIS 12b at 446 ka, in the lower MIS 12, at about 472 ka and 478 ka, and along with TVI at about 534 ka.

During MIS 12b the simultaneous peaks in the patterns of reworked nannofossils, *N. pachyderma* left coiling and lithics seem to support the occurrence of an additional H-type event; it is slightly preceded by peaks of *G. margereli-G. muellerae* >4 μm and *C. pelagicus pelagicus* as in the younger equivalents (Figures 4j and 4k). In the lower MIS 12 the cooccurrence of peaks of *G. margereli-G. muellerae* >4 μm, *N. pachyderma* left coiling, and reworked nannofossils, although less pronounced, could be similarly regarded as H-type events, in accordance

with simultaneous benthic $\delta^{13}C$ minima at the site (Figure 4b). It is noteworthy that the events occurring within the lower MIS 12 fall within an insolation minimum (Figure 4a), which may have favored a certain ice sheet stability and prevented significant iceberg delivery and IRD discharge at the core location, where lithics are not recorded. At the TVI the patterns of *C. pelagicus pelagicus*, reworked nannofossils, and *N. pachyderma* left coiling support the occurrence of a possible minor H-type event although no coarse-sized lithics have been recognized in the core. Nevertheless, it is worth to note that the contemporaneous insolation maximum at TVI is in line with the instability of ice sheets and possibly iceberg discharge related to insolation forcing. The absence of *G. margereli-G. muellerae* >4 μm during the H-type event at TVI could be related to the evolutionary factor since the taxon was not recorded in stratigraphic intervals older than MIS 12 and down to MIS 16 in the Mediterranean Sea [*Girone et al*., 2013] or to a less pronounced cooling. The extent of this cooling was not sufficient to enable important proliferation of *N. pachyderma* left coiling (Figure 4f).

The coccolithophore signals of the inferred additional H-type events are not always associated with lithics at the studied core and with analogous at Site U1313 (i.e., peaks of dolomite/calcite = IRD from the Hudson area, higher $C_{37:4}$ alkenones = high-latitude waters, SST minima); on the other hand, they always match synchronous IRD flux (from Greenland and Iceland ice sheets) at Site U1314 (Figures 4k–4m).

Although several factors may control the areal distribution of IRD and their chronology [*Hemming*, 2004], we believe that the coarse size fraction >315 μm considered for lithic fragments at the studied core may have only detected the major ice-rafting events with respect to the fraction >150 μm in size used at Site U1314 and usually employed for standard IRD analysis [*Hemming*, 2004]. Additionally, the main iceberg sources and the route path of icebergs depending on the regional Atlantic surface circulation [*Bond and Lotti*, 1995; *Alonso-Garcia et al*., 2011] could have played a role. On the basis of the correlation between our coccolithophore H-type signals at core MD01-2446 and IRD at the Site U1314, although with caution, a possible origin of icebergs from Greenland, Iceland, and Scandinavia rather than the Laurentide ice sheet could be invoked for the additional H-type events below TV. A European source (British ice sheet) is similarly suggested by *Rodrigues et al*. [2011] for some H-type events in the core MD03-2699 (Figure 4n), which records the H-type events Ht4 and Ht7 nearly synchronous with the H-type events recorded in core MD01-2446 in upper TIV and at 472 ka, respectively (Figure 4). Discrepancies in the chronology between the H-type events in core MD01-2446 and those recorded in core MD03-2699 (excluding Ht2 and Ht3) appear tolerable within the limits of the different age models.

6. Summary and Conclusion

The fluctuations of total coccolithophore abundance and of selected even rare taxa in core MD01-2446 reveal that significant changes in surface water features occurred at the glacial-interglacial cycles as well as on millennial scale. Total coccolithophore productivity (NAR) increased during interglacials in relation to more stable oligotrophic and warmer surface water condition. They also mimic the pattern of the $CaCO_3$ record revealing that coccoliths are the major contributor to carbonate production at the core location. However, dissolution and dilution processes have to be considered mainly during colder glacial phases and deglaciations. The influence of the STF, even though with different efficiency, is recorded during interglacials since surface waters were similarly warm during substages MIS 13c, 11c, and 9e as documented by the pattern of the warm-water coccolithophore cumulative curve (wwt). The three interglacials differ somewhat depending on water column stability and nutrient availability, and warming at the nutricline depth as well. MIS 13 is an unstable interglacial showing higher-frequency variation in the wwt and total NAR. The higher abundance of wwt during MIS 13c rather than during MIS 13a, the latter considered the full interglacial of MIS 13, is possibly related to instability and cooler condition in the middle to deep photic zone during MIS 13a. Furthermore, coccolithophore behavior suggests that the warming phase recorded during MIS 13c likely affected only surface waters. Differently, a more stratified water column characterized MIS 11c and 9e with higher temperature throughout the entire photic zone. A long-lasting warming occurred during MIS 11c when wwt recorded a time-expanded high abundance with respect to MIS 13c and 9e. A climate optimum during substage MIS 11c, with a more pronounced influence of the SFT at the site location with respect to MIS 9e, can be inferred, which is almost synchronous with the sea level highstand-warmth known at North Atlantic wide scale. The cold phases MIS 12 and 10 are characterized by higher percentages of the cool-cold water taxa *G. margereli-G. muellerae* 3–4 μm, possibly in relation to a more southern position of the polar front.

The pattern of wwt allowed recognition of distinct interstadial and stadial events during glacials and interglacials. These changes have a higher frequency during glacials (MIS 12 and 10) with respect to interglacials and have a duration ranging from 4 kyr to 10 kyr. Distinctive abundance peaks of the foraminifer *N. pachyderma* left coiling, larger morphotypes *G. margereli-muellerae* (>4 μm), and *C. pelagicus pelagicus* correlate with the four H-type events identified by *Voelker et al.* [2010] in MIS 10 (including TIV) and at TV based on the IRD pattern. Sharp abundance peaks of reworked calcareous nannofossils and minimum values in total NAR correlate with IRD. Based on these coccolithophore data, signals of additional H-type events are recorded at the core location, and they correspond with analogous H-type signals at Sites U1313 and U1314. Specifically, additional H-type events are indicated at about 446 ka within MIS 12b and at about 472 ka and 478 ka in the lower MIS 12. Furthermore, a minor H-type event is recorded at TVI at about 534 ka. The present results may represent an important contribution to the Iberian margin region where the new sites of IODP Expedition 339 allow extending the study further back in time.

Acknowledgments

G. Rothwell (Boscorf, UK) is greatly acknowledged for providing samples of Core MD01-2446. Valuable comments and critical suggestions by two anonymous reviewers and K.H. Baumann significantly improved the manuscript. This research was financially supported by Università di Bari: Fondi di Ateneo to R. La Perna, 2010 and PhD fellowship provided to F. Tarantino. A. Voelker acknowledges financial support from the Fundação para a Ciência e a Tecnologia (FCT) through the PORTO project (PDCT/MAR/58282/2004). This is ISMAR-CNR scientific contribution n. 1823.

References

Alonso-Garcia, M., F. J. Sierro, and J. A. Flores (2011), Arctic front shifts in the subpolar North Atlantic during the mid-Pleistocene (800–400 ka) and their implications for ocean circulation, *Palaeogeogr. Palaeoclimatol. Palaeoecol.*, *311*(3-4), 268–280, doi:10.1016/j.palaeo.2011.09.004.

Amore, F. O., J. A. Flores, A. H. L. Voelker, S. M. Lebreiro, E. Palumbo, and F. J. Sierro (2012), A Middle Pleistocene Northeast Atlantic coccolithophore record: Paleoclimatology and paleoproductivity aspects, *Mar. Micropaleontol.*, *90-91*, 44–59.

Archer, D., and E. Maier-Reimer (1994), Effect of deep-sea sedimentary calcite preservation on atmospheric CO_2 concentration, *Nature*, *367*, 260–263, doi:10.1038/367260a0.

Barker, S., D. Archer, L. Booth, H. Elderfield, J. Henderiks, and R. E. M. Rickaby (2006), Globally increased pelagic carbonate production during the mid-Brunhes dissolution interval and the CO_2 paradox of MIS 11, *Quat. Sci. Rev.*, *25*, 3278–3293.

Baumann, K.-H., and T. Freitag (2004), Pleistocene fluctuations in the northern Benguela Current system as revealed by coccolith assemblages, *Mar. Micropaleontol.*, *52*, 195–215.

Baumann, K.-H., H. Andruleit, and C. Samtleben (2000), Coccolithophores in the Nordic Seas: Comparison of living communities with surface sediment assemblages, *Deep Sea Res., Part II*, *47*, 1743–1772.

Baumann, K.-H., B. Bockel, and M. Frenz (2004), Coccolith contribution to South Atlantic carbonate sedimentation, in *Coccolithophores From Molecular Processes to Global Impact*, edited by H. R. Thierstein and J. Young, pp. 367–402, Springer, Berlin.

Baumann, K.-H., H. Andruleit, B. Böckel, M. Geisen, and H. Kinkel (2005), The significance of extant coccolithophores as indicators of ocean water masses, surface water temperature, and paleoproductivity: A review, *Paläontol. Z.*, *79*, 93–112.

Bé, A. W. H., and D. S. Tolderlund (1971), Distribution and ecology of living planktonic foraminifera in surface waters of the Atlantic and Indian Oceans, in *The Micropaleontology of the Oceans*, edited by B. M. Funnell and W. R. Riedel, pp. 105–149, Cambridge Univ. Press, London.

Beaufort, L., Y. Lancelot, P. Camberlin, O. Cayre, E. Vincent, F. Bassinot, and L. Labeyrie (1997), Insolation cycles as a major control of equatorial Indian Ocean primary production, *Science*, *278*, 1451–1454.

Beaufort, L., T. de Garidel-Thoron, A. C. Mix, and N. G. Pisias (2001), ENSO-like forcing on oceanic primary production during the late Pleistocene, *Science*, *293*, 2440–2444.

Berger, W. H., and G. Wefer (2003), On the dynamics of the ice ages: Stage-11 paradox, mid-Brunhes climate shift, and 100-ky cycle, in *Earths's Climate and Orbital Eccentricity: The Marine Isotope Stage 11 Question*, Geophysical Monograph Series, vol. 137, edited by A. W. Droxler, R. Z. Poore, and L. H. Burckle, pp. 41–59, AGU, Washington, D. C., doi:10.1029/137GM04.

Bintanja, R., R. S. W. van de Wal, and J. Oerlemans (2005), Modelled atmospheric temperatures and global sea levels over the past million years, *Nature*, *437*, 125–128.

Boeckel, B., and K.-H. Baumann (2004), Distribution of coccoliths in surface sediments of the south-eastern South Atlantic Ocean: Ecology, preservation and carbonate contribution, *Mar. Micropaleontol.*, *51*, 3101–3320.

Bollmann, J. (1997), Morphology and biogeography of Gephyrocapsa coccoliths in Holocene sediments, *Mar. Micropaleontol.*, *29*, 319–350.

Bond, G. C., and R. Lotti (1995), Iceberg discharges into the North Atlantic on millennial time scales during the last glaciation, *Science*, *267*, 1005–1010.

Bond, G. C., et al. (1992), Evidence for massive discharges of icebergs into the North Atlantic ocean during the last glacial, *Nature*, *360*, 245–249.

Bordiga, M., L. Beaufort, M. Cobianchi, C. Lupi, N. Mancin, V. Luciani, N. Pelosi, and M. Sprovieri (2013a), Calcareous plankton and geochemistry from the ODP site 1209B in the NW Pacific Ocean (Shatsky Rise): New data to interpret calcite dissolution and paleoproductivity changes of the last 450 ka, *Palaeogeogr. Palaeoclimatol. Palaeoecol.*, *371*, 93–108.

Bordiga, M., M. Cobianchi, C. Lupi, N. Pelosi, N. L. Venti, and P. Ziveri (2013b), Coccolithophore carbonate during the last 450 ka in the NW Pacific Ocean (ODP site 1209B, Shatsky Rise), *J. Quat. Sci.*, doi:10.1002/jqs.2677.

Bown, P. R., J. A. Lees, and J. R. Young (2004), Calcareous nannoplankton evolution and diversity through time, in *Coccolithophores—From Molecular Processes to Global Impact*, edited by H. R. Thierstein and J. R. Young, pp. 481–508, Springer, Berlin.

Broecker, W. S., G. Bond, J. F. McManus, M. Klas, and E. Clark (1992), Origin of the northern Atlantic's Heinrich events, *Clim. Dyn.*, *6*, 265–273.

Cacho, I., J. O. Grimalt, C. Pelejero, M. Canals, F. J. Sierro, J. A. Flores, and N. J. Shackleton (1999), Dansgaard-Oeschger and Heinrich event imprints in the Alboran Sea paleotemperatures, *Paleoceanography*, *14*, 698–705, doi:10.1029/1999PA900044.

Cacho, I., J. O. Grimalt, M. Canals, L. Sbaffi, N. J. Shackleton, J. Schoönfeld, and R. Zahn (2001), Variability of the western Mediterranean sea surface temperature during the last 25,000 years and its connection with the Northern Hemisphere climatic changes, *Paleoceanography*, *16*, 40–52, doi:10.1029/2000PA000502.

Chapman, M. R., and M. A. Maslin (1999), Low-latitude forcing of meridional temperature and salinity gradients in the subpolar North Atlantic and the growth of glacial ice sheets, *Geology*, *27*, 875–878.

Cléroux, C., E. Cortijo, J.-C. Duplessy, and R. Zahn (2007), Deep-dwelling foraminifera as thermocline temperature recorders, *Geochem. Geophys. Geosyst.*, *8*, Q04N11, doi:10.1029/2006GC001474.

Colmenero-Hidalgo, E., J. A. Flores, and F. J. Sierro (2002), Biometry of Emiliana huxleyi and its biostratigraphic significance in the eastern North Atlantic Ocean and western Mediterranean Sea in the last 20,000 years, *Mar. Micropaleontol.*, *46*, 247–263.
Colmenero-Hidalgo, E., J. A. Flores, F. J. Sierro, M. A. Barcena, L. Lowemark, J. Schonfeld, and J. O. Grimalt (2004), Ocean surface water response to short-term climate changes revealed by coccolithophores from the Gulf of Cadiz (NE Atlantic) and Alboran Sea (W Mediterranean), *Palaeogeogr. Palaeoclimatol. Palaeoecol.*, *205*, 317–336.
Cortes, M., J. Bollmann, and H. R. Thierstein (2001), Coccolithophore ecology at the HOT station ALOHA Hawaii, *Deep Sea Res., Part II*, *48*, 1947–1981.
Cros, L. (2001), Planktonic coccolithophores of the NW Mediterranean, Tesi Doctoral, Departament d'Ecologia, Universitat de Barcelona.
de Abreu, L., N. J. Shackleton, J. Schonfeld, M. Hall, and M. Chapman (2003), Millennial scale oceanic climate variability off the western Iberian margin during the last two glacial periods, *Mar. Geol.*, *196*, 1–20.
de Abreu, L., F. Abrantes, N. Shackleton, P. C. Tzedakis, J. F. McManus, D. W. Oppo, and M. A. Hall (2005), Ocean climate variability in the eastern North Atlantic during interglacial Marine Isotope Stage 11: A partial analogue for the Holocene?, *Paleoceanography*, *20*, PA3009, doi:10.1029/2004PA001091.
Deuser, W. G., and E. H. Ross (1989), Seasonally abundant planktonic-foraminifera of the Sargasso Sea—Succession, deep-water fluxes, isotopic compositions, and paleoceanographic implications, *J. Foraminiferal Res.*, *19*(4), 268–293.
Di Stefano, E., and A. Incarbona (2004), High resolution paleoenvironmental reconstruction of the ODP-963D Hole (Sicily Channel) during the last deglaciation, based on calcareous nannofossils, *Mar. Micropaleontol.*, *52*, 241–254.
Di Tullio, G. R., J. M. Grebmeier, K. R. Arrigo, M. P. Lizotte, D. H. Robinson, A. Leventer, J. P. Barry, M. L. Van Woert, and R. B. Dunbar (2000), Rapid and early export of Phaeocystis antarctica blooms in the Ross Sea, Antarctica, *Nature*, *404*, 595–598.
Dimiza, M. D., and M. V. Triantaphyllou (2010), Comparing living and Holocene coccolithophores assemblages in the Aegean marine environments, *Bull. Geol. Soc. Greece, 2010, XLIII*, *2*, 602–612.
Dittert, N., K.-H. Baumann, R. Bickert, R. Henrich, R. Huber, H. Kinkel, and H. Meggers (1999), Carbonate dissolution in the deep sea: Methods, quantification and paleoceanographic application, in *Use of Proxies in Paleoceanography: Examples From the South Atlantic*, edited by G. Fischer and G. Wefer, pp. 255–284, Springer Verlag, Berlin, Heidelberg.
Droxler, A. W., R. B. Alley, W. R. Howard, R. Z. Poore, and L. H. Burckle (2003), Unique and exceptionally long interglacial Marine Isotope Stage 11: Window into Earth warm future climate, in *Earth's Climate and Orbital Eccentricity: The Marine Isotope Stage 11 Question*, Geophysical Monograph, vol. 137, edited by A. W. Droxler, R. Z. Poore, and L. H. Burckle, pp. 1–14, AGU, Wash.
Flores, J. A., and F. J. Sierro (1997), Revised technique for calculation of calcareous nannofossil accumulation rates, *Micropaleontology*, *43*, 321–324.
Flores, J. A., F. J. Sierro, G. Francés, A. Vázquez, and I. Zamarrefio (1997), The last 100,000 years in the western Mediterranean: Sea surface water and frontal dynamics as revealed by coccolithophores, *Mar. Micropaleontol.*, *29*, 351–366.
Flores, J. A., R. Gersonde, F. J. Sierro, and H. S. Niebler (2000), Southern Ocean Pleistocene calcareous nannofossil events: Calibration with isotope and geomagnetic stratigraphies, *Mar. Micropaleontol.*, *40*, 377–402.
Flores, J. A., E. Colmenero-Hidalgo, A. E. Mejía-Molina, K.-H. Baumann, J. Henderiks, K. Larsson, C. N. Prabhu, F. J. Sierro, and T. Rodrigues (2010), Distribution of large Emiliania huxleyi in the Central and Northeast Atlantic as a tracer of surface ocean dynamics during the last 25,000 years, *Mar. Micropaleontol.*, *76*, 53–66.
Geisen, M., C. Billard, A. T. C. Broerse, L. Cros, I. Probert, and J. R. Young (2002), Life-cycle associations involving pairs of holococcolithophorid species: Intraspecific variation or cryptic speciation?, *Eur. J. Phycol.*, *37*, 531–550.
Giraudeau, J., M. Grelaud, S. Solignac, J. T. Andrews, M. Moros, and E. Jansen (2010), Millennial-scale variability in Atlantic water advection to the Nordic Seas derived from Holocene coccolith concentration records, *Quat. Sci. Rev.*, *29*, 1276–1287.
Girone, A., P. Maiorano, M. Marino, and M. Kucera (2013), Calcareous plankton response to orbital and millennial-scale climate changes across the Middle Pleistocene in the western Mediterranean, *Palaeogeogr. Palaeoclimatol. Palaeoecol.*, *392*, 105–116, doi:10.1016/j.palaeo.2013.09.005.
Hagino, K., and D. K. Kulhanek (2009), Data report: Calcareous nannofossils from upper Pliocene and Pleistocene, Expedition 306 Sites U1313 and U1314, in *Proceedings of the Integrated Ocean Drilling Program 303/306*, edited by J. E. T. Channell, et al., pp. 1925–1956, College Station, Tex., doi:10.2204/iodp.proc.303306.206.2009.
Haidar, A. T., and H. R. Thierstein (2001), Coccolithophore dynamics off Bermuda (N. Atlantic), *Deep Sea Res., Part II*, *48*, 1925–1956.
Hammer, Ø., D. A. T. Harper, and P. D. Ryan (2001), PAST: Paleontological statistics software package for education and data analysis, *Palaeontol. Electron.*, *4*(1, Article 4).
Helmke, J. P., H. A. Bauch, U. Röhl, and E. S. Kandiano (2008), Uniform climate development between the subtropical and subpolar Northeast Atlantic across Marine Isotope Stage 11, *Clim. Past Discuss.*, *4*, 433–457.
Hemleben, C., M. Spindler, and O. R. Anderson (1989), *Modern Planktonic Foraminifera*, Springer-Verlag, New York.
Hemming, S. R. (2004), Heinrich events: Massive late Pleistocene detritus layers of the North Atlantic and their global climate imprint, *Rev. Geophys.*, *42*, RG1005, doi:10.1029/2003RG000128.
Hodell, D. A., C. D. Charles, and U. S. Ninneman (2000), Comparison of interglacial stages in the South Atlantic sector of the southern ocean for the past 450 ka: Implications for Marine Isotope Stage (MIS) 11, *Global Planet. Change*, *24*(1), 7–26.
Hodell, D. A., K. A. Venz, C. D. Charles, and U. S. Ninnemann (2003), Pleistocene vertical isotope and carbonate gradient in South Atlantic sector of the Southern Ocean, *Geochem. Geophys. Geosyst.*, *4*(1), 1004, doi:10.1029/2002GC000367.
Hodell, D. A., J. E. T. Channell, J. H. Curtis, O. E. Romero, and U. Röhl (2008), Onset of "Hudson Strait" Heinrich events in the Eastern North Atlantic at the end of the middle Pleistocene transition (−640 ka)?, *Paleoceanography*, *23*, PA4218, doi:10.1029/2008PA001591.
Honjo, S., and H. Okada (1974), Community structure of coccolithophores in the photic layer of the mid-Pacific, *Micropaleontology*, *20*, 209–230.
Howard, W. R. (1997), A warm future in the past, *Nature*, *388*, 418–419.
Incarbona, A., et al. (2008), Calcareous nannofossil surface sediment assemblages from the Sicily Channel (central Mediterranean Sea): Palaeoceanographic implications, *Mar. Micropaleontol.*, *67*, 297–309.
Jansen, J. H. F., A. Kuijpers, and S. R. Troelstra (1986), A mid-Brunhes climatic event: Long-term changes in global atmospheric and ocean circulation, *Science*, *232*, 619–622.
Johannessen, T., E. Jansen, A. Flatoy, and A. C. Ravelo (1994), The relationship between surface water masses, oceanographic fronts and paleoclimatic proxies in surface sediments of the Greenland Iceland and Norwegian seas, in *Carbon Cycling in the Glacial Ocean: Constraints on the Ocean's Role in Global Change*, NATO Asi Series, I, vol. 17, edited by R. Zahn et al., pp. 61–85, Springer, New York.
Jouzel, J., et al. (2007), Orbital and millennial Antarctic climate variability over the past 800,000 years, *Science*, *317*, 793–796.
Kandiano, E. S., H. A. Bauch, K. Fahl, J. P. Helmke, U. Röhl, M. Pérez-Folgado, and I. Cacho (2012), The meridional temperature gradient in the eastern North Atlantic during MIS11 and its link to the ocean–atmosphere system, *Palaeogeogr. Palaeoclimatol. Palaeoecol.*, *333-334*, 24–39.

Kinkel, H., K.-H. Baumann, and M. Čepek (2000), Coccolithophores in the equatorial Atlantic Ocean: Response to seasonal and late Pleistocene surface water variability, *Mar. Micropaleontol.*, *39*, 87–112.
Kulhanek, D. K. (2009), Calcareous nannoplankton as paleoceanographic and biostratigraphic proxies: Examples from the mid-Cretaceous equatorial Atlantic (ODP leg 207) and Pleistocene of the Antarctic Peninsula (NBP0602A) and North Atlantic (IODP Exp. 306), PhD Dissertation, Florida State Univ., College of Arts and Sciences.
Kulhanek, D. K., A. H. Voelker, and J. Grützner (2008), Centennial-scale nannoplankton productivity changes in the mid-latitude North Atlantic during Marine Isotope Stages 11–12: Evidence from IODP site 1313, Abstract PP11B-1395 presented at Fall Meeting 2008, AGU.
Lang, N., and E. W. Wolff (2011), Interglacial and glacial variability from the last 800 ka in marine, ice and terrestrial archives, *Clim. Past*, *7*, 361–380, doi:10.5194/cp-7-361-2011.
Laskar, J., P. Robutel, F. Joutel, M. Gastineau, A. C. M. Correia, and B. Levrard (2004), A long-term numerical solution of the insolation quantities of the Earth, *Astron. Astrophys.*, *428*(261–285), 2004.
Lebreiro, S. M., J. C. Moreno, F. F. Abrantes, and U. Pflaumann (1997), Productivity and paleoceanographic implications on the Tore Seamount (Iberian Margin) during the last 225 kyr: Foraminiferal evidence, *Paleoceanography*, *12*, 718–727, doi:10.1029/97PA01748.
Lisiecki, L. E., and M. E. Raymo (2005), A Pliocene-Pleistocene stack of 57 globally distributed benthic δ^{18}O records, *Paleoceanography*, *20*, PA1003, doi:10.1029/2004PA001071.
Loutre, M. F., and A. Berger (2003), Marine Isotope Stage 11 as an analogue for the present interglacial, *Global Planet. Change*, *36*, 209–217.
Lüthi, D., et al. (2008), High-resolution carbon dioxide concentration record 650 000–800 000 years before present, *Nature*, *453*, 379–382.
Maiorano, P., F. Tarantino, M. Marino, and A. Girone (2013a), A paleoecological and paleobiogeographic evaluation of Helicosphaera inversa (Gartner) Theodoridis and the diachrony of its first occurrence, *Mar. Micropaleontol.*, *104*, 14–24, doi:10.1016/j.marmicro.2013.08.001.
Maiorano, P., F. Tarantino, M. Marino, and G. J. De Lange (2013b), Paleoenvironmental conditions at Core KC01B (Ionian Sea) through MIS 13-9: Evidence from calcareous nannofossil assemblages, *Quat. Int.*, *288*, 97–111.
Marino, M., P. Maiorano, F. Lirer, and N. Pelosi (2009), Response of calcareous nannofossil assemblages to paleoenvironmental changes through the mid-Pleistocene revolution at Site 1090 (Southern Ocean), *Palaeogeogr. Palaeoclimatol. Palaeoecol.*, *280*, 333–349.
Marino, M., P. Maiorano, and B. P. Flower (2011), Calcareous nannofossil changes during the mid-Pleistocene Revolution: Paleoecologic and paleoceanographic evidence from North Atlantic Site 980/981, *Palaeogeogr. Palaeoclimatol. Palaeoecol.*, *306*, 58–69.
Marlowe, I. T., S. C. Brassell, G. Eglinton, and J. C. Green (1990), Long-chain alkenones and alkyl alkenoates and the fossil coccolith record of marine sediments, *Chem. Geol.*, *88*, 349–375.
Martrat, B., J. O. Grimalt, N. J. Shackleton, L. De Abreu, M. A. Hutterli, and T. F. Stocker (2007), Four climate cycles of recurring deep and surface water destabilizations on the Iberian margin, *Science*, *317*, 502–507, doi:10.1126/science.1139994.
Matsuoka, H. (1990), A new method to evaluate dissolution of $CaCO_3$ in the deep-sea sediments, *Trans. Proc. Palaeontol. Soc. Jpn.*, *157*, 430–434.
McIntyre, A., and A. H. W. Bè (1967), Modern coccolithophores of the Atlantic Ocean—I. Placolith and cyrtoliths, *Deep Sea Res.*, *14*, 561–597.
McIntyre, A., and B. Molfino (1996), Forcing of Atlantic equatorial and subpolar millennial cycles by precession, *Science*, *274*, 1867–1870, doi:10.1126/science.274.5294.1867.
McManus, J. F., D. W. Oppo, and J. L. Cullen (1999), A 0.5 million year record of millennial-scale climate variability in the North Atlantic, *Science*, *283*(5404), 971–975, doi:10.1126/science.283.5404.971.
McManus, J. F., D. Oppo, J. Cullen, and S. Healey (2003), Marine Isotope Stage 11 (MIS 11): Analog for Holocene and future climate?, in *Earth's Climate and Orbital Eccentricity: The Marine Isotope Stage 11 Question*, Geophys. Monograph. Ser., vol. 137, edited by A. W. Droxler, R. Z. Poore, and L. H. Burckle, pp. 69–86, AGU, Washington, D. C.
Molfino, B., and A. McIntyre (1990a), Precessional forcing of nutricline dynamics in the equatorial Atlantic, *Science*, *249*, 766–769.
Molfino, B., and A. McIntyre (1990b), Nutricline variation in the equatorial Atlantic coincident with the Younger Dryas, *Paleoceanography*, *5*, 997–1008, doi:10.1029/PA005i006p00997.
Munhoven, G. (2007), Glacial–interglacial rain ratio changes: Implications for atmospheric CO_2 and ocean–sediment interaction, *Deep Sea Res., Part II*, *54*, 722–746.
Naafs, B. D. A., R. Stein, J. Hefter, N. Khèlifi, S. De Schepper, and G. H. Haug (2010), Late Pliocene changes in the North Atlantic Current, *Earth Planet. Sci. Lett.*, *298*(3-4), 434–442, doi:10.1016/j.epsl.2010.08.023.
Naafs, B. D. A., J. Hefter, P. Ferretti, R. Stein, and G. H. Haug (2011), Sea surface temperatures did not control the first occurrence of Hudson Strait Heinrich events during MIS 16, *Paleoceanography*, *26*, PA4201, doi:10.1029/2011PA002135.
Naafs, B. D. A., J. Hefter, G. Acton, G. H. Haug, A. Martínez-Garcia, R. Pancost, and R. Stein (2012), Strengthening of North American dust sources during the late Pliocene (2.7 Ma), *Earth Planet. Sci. Lett.*, *317-318*, 8–19, doi:10.1016/j.epsl.2011.11.026.
Naafs, B. D. A., J. Hefter, and R. Stein (2013), Millennial-scale ice rafting events and Hudson Strait Heinrich(-like) events during the late Pliocene and Pleistocene: A review, *Quat. Sci. Rev.*, *80*, 1–28, doi:10.1016/j.quascirev.2013.08.014.
Nave, S., S. Lebreiro, C. Kissel, A. Guihou, M. O. Figueiredo, T. P. Silva, E. Michel, E. Cortijo, L. Labeyrie, and A. Voelker (2010), Open oceanic productivity changes at mid-latitudes during interglacials and its relation to the Atlantic meridional overturning circulation, *Geophys. Res. Abstr.*, *12*, EGU2010-14696-1. EGU General Assembly 2010.
Okada, H., and S. Honjo (1973), The distribution of oceanic coccolithophorids in the Pacific, *Deep Sea Res.*, *20*, 355–374.
Okada, H., and A. McIntyre (1979), Seasonal distribution of modern coccolithophores in the western North Atlantic Ocean, *Mar. Biol.*, *54*, 319–328.
Okada, H., and P. Wells (1997), Late Quaternary nannofossil indicators of climate change in two deep-sea cores associated with the Leeuwin Current off Western Australia, *Palaeogeogr. Palaeoclimatol. Palaeoecol.*, *131*, 413–432.
Oppo, D. W., and S. J. Lehman (1993), Mid-depth circulation of the subpolar North Atlantic during the Last Glacial Maximum, *Science*, *259*, 1148–1152.
Oppo, D. W., J. McManus, and J. C. Cullen (1998), Abrupt climate change events 500 000 to 340 000 years ago: Evidence from subpolar North Atlantic sediments, *Science*, *279*, 1335–1338.
Oppo, D. W., L. D. Keigwin, J. F. McManus, and J. L. Cullen (2001), Persistent suborbital climate variability in Marine Isotope Stage 5 and termination II, *Paleoceanography*, *16*, 280–292, doi:10.1029/2000PA000527.
Palumbo, E., J. A. Flores, C. Perugia, Z. Petrillo, A. H. L. Voelker, and F. O. Amore (2013), Millennial scale coccolithophore paleoproductivity and surface water changes between 445 and 360 ka (Marine Isotope Stages 12/11) in the northeast Atlantic, *Palaeogeogr. Palaeoclimatol. Palaeoecol.*, *383-384*, 27–41.
Parente, A., M. Cachão, K.-H. Baumann, L. de Abreu, and J. Ferreira (2004), Morphometry of Coccolithus pelagicus s.l. (Coccolithophore, Haptophyta) from offshore Portugal, during the last 200 kyr, *Micropaleontology*, *50*, 107–120.

Peliz, A., J. Dubert, A. M. P. Santos, P. B. Oliveira, and B. Le Cann (2005), Winter upper ocean circulation in the Western Iberian Basin—Fronts, Eddies and Poleward Flows: An overview, *Deep Sea Res., Part I*, *52*, 621–646.

Perez-Folgado, M., F. J. Sierro, J. A. Flores, I. Cacho, J. O. Grimalt, R. Zahn, and N. Shackleton (2003), Western Mediterranean planktonic foraminifera events and millennial climatic variability during the last 70 kyr, *Mar. Micropaleontol.*, *48*, 49–70.

Pflaumann, U., et al. (2003), Glacial North Atlantic: Sea-surface conditions reconstructed by GLAMAP 2000, *Paleoceanography*, *18*(3), 1065, doi:10.1029/2002PA000774.

Raffi, I., J. Backman, E. Fornaciari, H. Pälike, D. Rio, L. Lourens, and F. Hilgen (2006), A review of calcareous nannofossil astrobiochronology encompassing the past 25 million years, *Quat. Sci. Rev.*, *25*, 3113–3137.

Raymo, M. E., D. W. Oppo, and W. Curry (1997), The mid-Pleistocene climate transition: A deep sea carbon isotopic perspective, *Paleoceanography*, *12*, 546–559, doi:10.1029/97PA01019.

Raymo, M. E., D. W. Oppo, B. P. Flower, D. A. Hodell, J. McManus, K. A. Venz, K. F. Kleiven, and K. McIntyre (2004), Stability of North Atlantic water masses in face of pronounced climate variability during the Pleistocene, *Paleoceanography*, *19*, PA2008, doi:10.1029/2003PA000921.

Reynolds, L. A., and R. C. Thunell (1986), Seasonal production and morphologic variation of Neogloboquadrina pachyderma (Ehrenberg) in the northeast Pacific, *Micropaleontology*, *32*, 1–18.

Rodrigues, T., A. H. L. Voelker, J. O. Grimalt, F. Abrantes, and F. Naughton (2011), Iberian Margin sea surface temperature during MIS 15 to 9 (580–300 ka): Glacial suborbital variability versus interglacial stability, *Paleoceanography*, *26*, PA1204, doi:10.1029/2010PA001927.

Rohling, E. J., A. Hayes, S. De Rijk, D. Kroon, W. J. Zachariasse, and D. Eisma (1998), Abrupt cold spells in the northwest Mediterranean, *Paleoceanography*, *13*, 316–322, doi:10.1029/98PA00671.

Ruddiman, W. F. (1977), Late Quaternary deposition of ice rafted sand in the subpolar North Atlantic, *Geol. Soc. Am. Bull.*, *83*, 2817–2836.

Saavedra-Pellitero, M., J. A. Flores, K.-H. Baumann, and F. J. Sierro (2010), Coccolith distribution patterns in surface sediments of equatorial and southeastern Pacific Ocean, *Geobios*, *43*, 131–149, doi:10.1016/j.geobios.2009.09.004.

Salgueiro, E., A. H. L. Voelker, L. de Abreu, F. Abrantes, H. Meggers, and G. Wefer (2010), Temperature and productivity changes off the western Iberian margin during the last 150 ky, *Quat. Sci. Rev.*, *29*, 680–695.

Samtleben, C., and T. Bickert (1990), Coccoliths in sediment traps from the Norwegian Sea, *Mar. Micropaleontol.*, *16*, 39–64.

Sierro, F. J., et al. (2005), Impact of iceberg melting on Mediterranean thermohaline circulation during Heinrich events, *Paleoceanography*, *20*, PA2019, doi:10.1029/2004PA001051.

Sigman, D. M., D. C. McCorkle, and W. R. Martin (1998), The calcite lysocline as a constraint on glacial/interglacial low-latitude production changes, *Global Biogeochem. Cycles*, *12*, 409–427, doi:10.1029/98GB01184.

Sorrosa, J. M., M. Satoh, and Y. Shiraiwa (2005), Low temperature stimulates cell enlargement and intracellular calcification of coccolithophorids, *Mar. Biotechnol.*, *7*, 128–133.

Stein, R., J. Hefter, J. Grützner, A. Voelker, and B. D. A. Naafs (2009), Variability of surface water characteristics and Heinrich-like events in the Pleistocene midlatitude North Atlantic Ocean: Biomarker and XRD records from IODP Site U1313 (MIS 16–9), *Paleoceanography*, *24*, PA2203, doi:10.1029/2008PA001639.

Steinmetz, J. C. (1994), Sedimentation of coccolithophores, in *Coccolithophores*, edited by A. Winter and W. G. Siesser, pp. 179–197, Cambridge Univ. Press, London.

Stolz, K., and K. H. Baumann (2010), Changes in palaeoceanography and palaeoecology during Marine Isotope Stage (MIS) 5 in the eastern north Atlantic (ODP site 980) deduced from calcareous nannoplankton observations, *Palaeogeogr. Palaeoclimatol. Palaeoecol.*, *292*, 295–305.

Tortell, P. D., G. R. Di Tullio, D. M. Sigman, and F. M. M. Morel (2002), CO_2 effects on taxonomic composition and nutrient utilization in an equatorial Pacific phytoplankton assemblage, *Mar. Ecol. Prog. Ser.*, *236*, 37–43.

Tzedakis, P. C. (2010), The MIS 11-MIS 1 analogy, southern European vegetation, atmospheric methane and the early anthropogenic hypothesis, *Clim. Past*, *6*, 131–144.

Tzedakis, P. C., et al. (1997), Comparison of terrestrial and marine records of changing climate of the last 500 000 years, *Earth Planet. Sci. Lett.*, *150*, 171–176.

Tzedakis, P. C., H. Hooghiemstra, and H. Palike (2006), The last 1.35 million years at Tenaghi Philippon: Revised chronostratigraphy and long-term vegetation trends, *Quat. Sci. Rev.*, *25*, 3416–3430.

Villanueva, J., J. O. Grimalt, E. Cortijo, L. Vidal, and L. Labeyrie (1997), A biomarker approach to the organic matter deposited in the North Atlantic during the last climatic cycle, *Geochim. Cosmochim. Acta*, *61*, 4633–4646.

Villanueva, J., E. Calvo, C. Pelejero, J. O. Grimalt, A. Boelaert, and L. Labeyrie (2001), A latitudinal productivity band in the central North Atlantic over the last 270 kyr: An alkenone perspective, *Paleoceanography*, *16*, 617–625.

Voelker, A. H. L., and L. de Abreu (2011), A review of abrupt climate change events in the northeastern Atlantic ocean (Iberian margin): Latitudinal, longitudinal and vertical gradients, in *Abrupt Climate Change: Mechanisms, Patterns, and Impacts*, edited by H. Rashid, L. Polyak, and E. Mosley-Thompson, pp. 15–37, AGU, Washington D. C.

Voelker, A. H. L., S. M. Lebreiro, J. Schönfeld, I. Cacho, H. Erlenkeuser, and F. Abrantes (2006), Mediterranean outflow strengthening during northern hemisphere coolings: A salt source for the glacial Atlantic?, *Earth Planet. Sci. Lett.*, *245*(1–2), 39–55.

Voelker, A. H. L., L. de Abreu, J. Schönfeld, H. Erlenkeuser, and F. Abrantes (2009), Hydrographic conditions along the western Iberian margin during Marine Isotope Stage 2, *Geochem. Geophys. Geosyst.*, *10*, Q12U08, doi:10.1029/2009GC002605.

Voelker, A. H. L., T. Rodrigues, K. Billups, D. Oppo, J. McManus, R. Stein, J. Hefter, and J. O. Grimalt (2010), Variations in mid-latitude North Atlantic surface water properties during the mid-Brunhes (MIS 9–14) and their implications for the thermohaline circulation, *Clim. Past*, *6*, 531–552.

Weaver, P. P. E., and C. Pujol (1988), History of the last deglaciation in the Alboran Sea (western Mediterranean) and adjacent North Atlantic as revealed by coccolith floras, *Palaeogeogr. Palaeoclimatol. Palaeoecol.*, *64*, 35–42.

Wells, P., and H. Okada (1997), Response of nannoplankton to major changes in sea-surface temperature and movements of hydrological fronts over Site DSDP 594 (south Chatham Rise, southeastern New Zealand), during the last 130 kyr, *Mar. Micropaleontol.*, *32*(3-4), 341–363.

Winter, A., R. W. Jordan, and P. H. Roth (1994), Biogeography of living coccolithophores in ocean waters, in *Coccolithophores*, edited by A. Winter and W. G. Siesser, pp. 161–178, Cambridge Univ. Press, London.

Ziveri, P., R. C. Thunell, and D. Rio (1995), Export production of coccolithophores in an upwelling region: Results from San Pedro Basin, Southern California Borderlands, *Mar. Micropaleontol.*, *24*, 335–358.

Ziveri, P., K.-H. Baumann, B. Boeckel, J. Bollmann, and J. Young (2004), Biogeography of selected Holocene coccoliths in the Atlantic Ocean, in *Coccolithophores: From Molecular Processes to Global Impact*, edited by H. R. Thierstein and Y. R. Young, pp. 403–428, Springer, Berlin.